ARTICLE

OASYS: A novel FRET-based microfluidic device to aid MDD diagnosis

Aabha P Shams, Abhinand Lal, Anugraha M, Hana Lukman, Navaneeth K, Nayana Harilal, Priyanshi Srivastava, Ruchi Arya, Roshida M, Samiksha P, Sarthak Thorat, Suryasis Dutta, Umashankar Chellam, Vibhavari Medepalli, Vignesh Jayan, Yaswanth OS

Indian Institute of Science Education and Research, Thiruvananthapuram, India
Contact for correspondence: IISER TVM, Email: igem@iisertvm.ac.in.

Abstract

Major Depressive Disorder (MDD) is a prevalent mental health condition. The current methods of diagnosis of MDD mainly consist of self-report questionnaires, usually followed by clinical interviews, often relying on symptoms reported by the patient or the people around them. Understanding its underlying biological mechanisms requires precise and efficient analytical tools. OASYS is a novel and objective FRET (Förster or fluorescence resonance energy transfer) - based microfluidic device that quantifies and analyses biomarkers such as neurotransmitters, microRNAs, hormones, and proteins in human peripheral blood serum. OASYS helps in the simultaneous analysis of crucial blood biomarkers associated with MDD. The targeted biomarkers include microRNA-132 and microRNA-124, cortisol, serotonin, and dopamine. The microfluidic chip integrates advanced technologies, employing aptamers as highly selective molecular recognition elements and magnetic nanoprobes for enhanced sensitivity and quantification. The microfluidic platform provides several advantages, including rapid analysis, reduced sample volumes, and improved sensitivity compared to conventional methods. Our hardware includes a detection system with an Arduino UNO setup with an LCD screen. The fluorescence emitted by each biomarker is detected by a different photodarlington sensor and displayed on the screen. The simultaneous measurement of multiple biomarkers allows for a more comprehensive understanding of the neurobiological processes associated with MDD, potentially leading to improved diagnostic accuracy and personalized treatment approaches.

Keywords: Major Depressive Disorder, blood biomarkers, microfluidic chip, bioengineering, synthetic biology

Graphical abstract

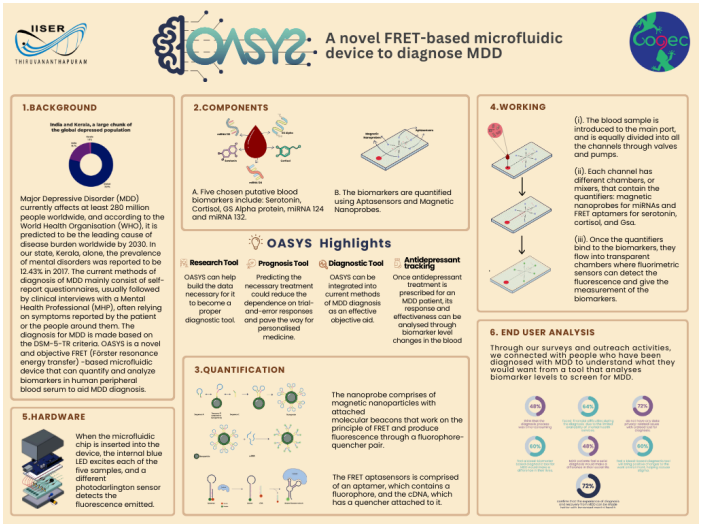

Figure 1: Graphical representation of the working of OASYS

Background

Major depressive disorder (MDD), or clinical depression, is a complex and heterogeneous clinical syndrome characterised by persistently depressed moods, loss of interest in daily activities and physical symptoms according to the widely used DSM-5-TR criteria[1]. It currently affects at least 280 million people worldwide[2], and according to the World Health Organisation (WHO), it is predicted to be the leading cause of disease burden worldwide by 2030 [3].

In our state, Kerala, alone, the prevalence of mental disorders was reported to be 12.43% in 2017. The number of individuals with mental health illnesses in the state increased from 272 per 100,000 to 400 people per 100,000 from 2002 to 2018[4]. The COVID-19 pandemic has profoundly impacted mental health in Kerala and globally.

The current methods of diagnosis of MDD mainly consist of self-report questionnaires, which are usually followed by clinical interviews with a Mental Health Professional (MHP), often relying on symptoms reported by the patient or the people around them, and the diagnosis for MDD is made based on the DSM-5-TR criteria[5]. These methods could be subjective and prone to variability, and this could lead to misdiagnosis. Patients and the people around them are often ignorant of depression and other mental illnesses as diseases and are hesitant to accept their diagnosis. There is a need for an objective and sensitive point-of-care diagnostic aid for clinical depression. Through OASYS, we hope to offer an objective aid to simplify the process of MDD diagnosis by reducing the dependence on self-reported symptoms and making it time and effort-efficient for the patients.

Project Design

OASYS is a novel and objective FRET (Förster or fluorescence resonance energy transfer)--based microfluidic device that can quantify and analyse biomarkers such as neurotransmitters, microRNAs, hormones, and proteins in human peripheral blood

serum. This device can be used as an objective aid to diagnose Major Depressive Disorder (MDD).

Five putative blood biomarkers correlated to MDD were chosen through a Bayesian analysis: *Neurotransmitter - Serotonin, Hormone - Cortisol, Protein - Gsα subunit*, *miRNA 124 & miRNA 132*. Along with this, we developed two quantification methods - Aptasensors for serotonin, cortisol and the Gsα protein, and Magnetic Nanoprobes, used for the microRNAs, that work on the principles of FRET, producing fluorescence whose readouts can relate to the blood biomarker levels.

These quantification systems are incorporated into a microfluidic chip that can take blood samples as input and run the assays simultaneously. We built a hardware system with fluorometric sensors that can detect the fluorescence produced by the chip to analyse and estimate the biomarker concentrations.

The Quantifiers

***Aptasensors*:** Aptamers are artificially synthesised single-stranded DNA or RNA sequences that can easily change conformations, allowing them to bind to specific targets with high affinity. Hence, they can be used in biosensing for clinical diagnostics. FRET is a non-radiative energy transfer process that occurs over small-scale separations (usually in nanometers) between an emitter (donor) and an absorber molecule (acceptor), often called a 'FRET' pair. We have chosen 6-FAM and Iowa Black FQ as the donor-acceptor FRET pair.

The FRET aptasensors comprise an aptamer, which contains a fluorophore, and the cDNA, which has a quencher attached to it. While the cDNA is bound to the aptamer, the fluorophores transfer energy to the quencher, and fluorescence is not observed. However, in the presence of the target, the FRET aptamers bind to it, displacing the cDNA. The fluorophore will produce a detectable fluorescent signal with no quencher in the vicinity. These FRET aptamers quantify the neurotransmitter serotonin, the hormone cortisol, and the Gsα protein[6].

We synthesized two aptamers targeting cortisol (85 nucleotides and 14 nucleotides in length) and one aptamer specific to serotonin (44 nucleotides in length). Additionally, we formulated two distinct complementary DNA (cDNA) sequences for the 85-nucleotide cortisol aptamer and the serotonin aptamer. The cDNA designs were crafted using partial complementarity for one version and another version based on the binding affinity (kD value) of the aptamer-cDNA pair. All sequences were procured through Integrated DNA technologies.

Magnetic Nanoprobes: Nanoprobes are small, nano-sized devices that interact with a biomolecule and can be used for diagnostic purposes. Our nanoprobe consists of magnetic nanoparticle with attached molecular beacons that work on the principle of FRET and produce fluorescence through a fluorophore-quencher pair. The molecular beacons are single-stranded DNA structures with three prominent parts: one complementary to the target miRNA, one attached to a fluorophore, and one to a quencher.

When inert, the nanoprobe exists in a hairpin structure, and the probe holds the quencher near the fluorophore, thus emitting no signal. When the target miRNA binds to the probe, the target-probe hybridisation can open the hairpin, forming an active "Y" structure. This active structure separates the fluorophore and the quencher, emitting fluorescence. The detection of the miRNAs, present in lower concentrations in the blood, is further enhanced by attaching the molecular beacons to magnetic nanoparticles to focus fluorescence on a smaller area[7].

The experiments were conducted using miDNAs as a working model owing to the unstable nature of miRNAs. The FASTA sequences for miRNA-124 and miRNA-132 was obtained from the microRNA database miRBase. The miDNA sequences were procured through Integrated DNA technologies.

Microfluidic Chip

We intend to design a PolyDiMethylSiloxane (PDMS) based microfluidic chip that uses human blood samples as the input and incorporates all the quantification systems for the biomarkers, involving five channels. The blood sample is introduced to the main port, which is equally divided into all the channels through valves and pumps. Each channel has different chambers, or mixers, that contain the quantifiers: magnetic nanoprobes for miRNAs and FRET aptasensors for serotonin, cortisol, and Gsα protein. These mixers are chosen based on the specific conditions required for the quantifier to attach to the biomarkers. Once the quantifiers bind to the biomarkers, they are flown into transparent chambers where fluorimetric sensors can detect the fluorescence and give a measurement of the biomarkers [6].

Detection System

The detection system consists of a 3D-printed box equipped with an LCD screen, an Arduino UNO setup, and the necessary accessories. When the microfluidic chip is inserted into the device, the internal blue LED excites each of the five samples, and the fluorescence emitted is detected by a different photodarlington sensor. The measured fluorescence intensity is then converted into the biomarker concentration levels and displayed on the LCD screen, with all data readings managed by the Arduino UNO microcontroller.

Results

Nanoprobes

Characterization: We successfully characterised the nanoparticle by zeta potential and TEM analyses. The presence of a carboxyl group was confirmed, and the size was estimated to be up to 12 nm. Detailed protocols and related data can be found in the supplementary material.

Native polyacrylamide gel electrophoresis: This was done to verify the formation of the probes and their binding to the miDNAs. The bands in the native page given are in the following order from the left (Fig 3.B and 3.C):

Sequence A (2), sequence B (3), sequence C (4), Sequence A+B (5), Sequence A+B+C {incubated for 1 hour (1:1:3 ratio) to form the probe} (6), Probe + miDNA (7).

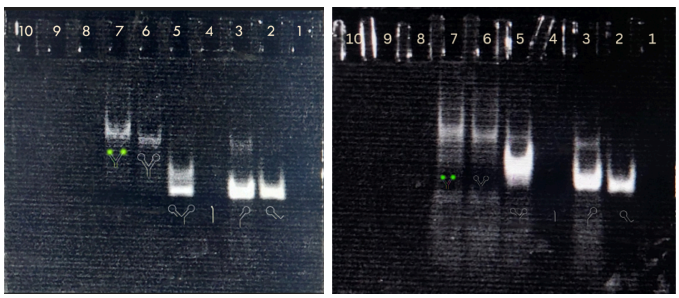

Figure 2: (A) Gel (12%) image verifying probe formation and miDNA binding for probe 132 (B) Gel (12%) image verifying probe formation and miDNA binding for probe 124.

The bands of sequences A and B are at the same level, indicating the same number of nucleotides. The A+B lane is higher than the A and B lanes, but the band is smeared. This is because A and B are only partially complementary, and they will not bind and form a stable structure. The lane with A+B+C (which forms the probe) has just one band, which is higher than the A+B band, indicating that these three sequences are being bound together by complementarity and forming a stable structure. The band in the lane of 'probe + miDNA' is slightly higher than the band in the lane with just the probe, indicating that the miDNA is indeed binding to the probe. The difference is only small because the miDNA is just 22 nucleotides long.

Fluorescence-based experiments using microplate reader: For all the following experiments, the percentage change in fluorescence intensity was calculated by:

Percentage change in fluorescence intensity =

$$[(FI_s - FI_c)/FI_c] * 100$$

Where FI_s = fluorescence intensity of the sample and FI_c = fluorescence intensity of the control.

From Fig 3, the maximum percentage change observed was 19%. This was mainly because of the large background noise present due to the unbound A or B sequence, which had fluorophores attached to it.. It still showed that there was an increase in fluorescence intensity on the binding of miDNA in both 124 and 132 probes, proving that the binding of miDNA is causing the loop to open and separate the fluorophore quencher-pair. The background noise could only be removed after binding the probes to the nanoparticle.

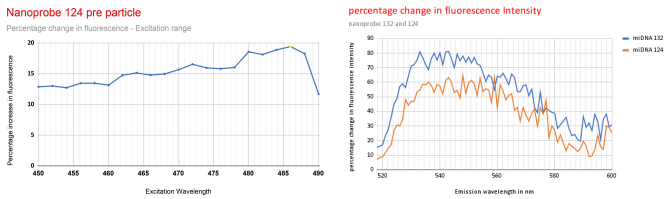

Figure 3: (A) graph representing percentage change in fluorescence intensity across different excitation wavelengths for 124 probes bound to miDNA 124. (B) Figure showing the percentage change in fluorescence intensity across different emission wavelengths for nanoprobe 132 and nanoprobe 124 bound to their respective miDNA

To test the fluorescence intensity change on adding the miDNA to the nanoprobe (after attachment), the fluorescence intensity change of the new nanoprobes was first measured (Fig 5.D). We conducted an emission scan with a constant excitation of 490 nm and an emission range of 500 nm - 600 nm. A maximum percentage increase of 81% was observed.

Comparing the results before and after attachment of the probe to the nanoparticle to form the nanoprobe:

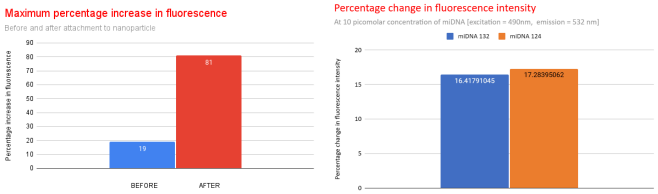

Figure 4: (A) Shows the maximum percentage increase in fluorescence observed before and after the probes were attached to the magnetic nanoparticle. (B) Figure showing the percentage change in fluorescence intensity at 532 nm wavelength emission for nanoprobe 132 and nanoprobe 124 bound to their respective miDNA present in 10 picomolar concentrations.

Results from Fig 4.A indicates that the nanoprobes give better fluorescence intensity change when compared to just probes.

The experiment was repeated to check the lowest concentration of detection by the nanoprobe. A fluorescence intensity change above 15% was observed for 10 picomolar (pm) concentrations of miDNA, proving that the nanoprobes can detect the low concentrations of miDNA in the sample without any amplification. The lower increase in fluorescence intensity when compared to samples of larger concentrations shows a direct correlation between the increase in fluorescence intensity and the increase in miDNA concentration. This shows that the method can be used for quantification.

At the range of 530 nm - 533 nm, both the probes showed similar percentage changes in fluorescence intensity with values close to 15%.

Specificity experiments: We tested the fluorescence intensity change in 4 different samples to test the specificity of the probe. The samples were:

Sample 1: with the 25 microliter probe and 75 microliter buffer as control. Sample 2: with 25 microliter probe and 75 microliter target miDNA. Sample 3: with 25 microliter probe and 75 microliter miDNA with just two nucleotide differences to the target miDNA. Sample 4: with 25 microliter probe and 75 microliter miDNA, completely different from the target miDNA. (All the miDNA used was of 10 nanomolar concentration).

The percentage change in fluorescence intensity was calculated using the fluorescence intensity of control as the base value.

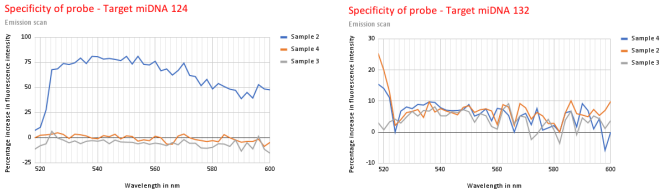

Figure 5 : (A) Figure showing the percentage change in fluorescence intensity across different emission wavelengths for three different samples. Sample 2 = 124 nanoprobe + miDNA 124, sample 3 = 124 nanoprobe + miDNA 124 sequence with two nucleotide differences, sample 4 = 124 nanoprobe + miDNA 132 (B) Figure showing the percentage change in fluorescence intensity across different emission wavelengths for three different samples. Sample 2 = 132 nanoprobe + miDNA 132, sample 3 = 132 nanoprobe + miDNA 132 sequence with 2 nucleotide difference, sample 4 = 132 nanoprobe + miDNA 124.

From Fig 5. A, the change in fluorescence intensity is close to 78% for the sample with the target miDNA, proving that the experimental conditions were optimal for the binding of miDNA.

Both the non-target miDNA 132 and the miDNA with just two nucleotide differences to the target miDNA 124 sequence showed no significant increase in fluorescence intensity. This shows that the nanoprobe 124 is highly specific to its target.

The experiment to study the specificity of miDNA 132 did not provide a reliable conclusion. This may be due to errors in the preparation of miDNA samples or nanoprobes.

APTASENSORS

Native PAGE

This experiment aimed to detect the hybridised complex of cDNA1 and the 85-mer aptamer. No clear indication of hybridisation could be derived from the native PAGE result, this could be due to the small size of our aptamer and cDNA. The experiment used a 12% gel, and similar results were seen. As seen in Fig 6.A, The only band was observed for 85-mer aptamer plus cortisol, we presume the cDNA 2, which is a 15-mer, had run off the gel.

Fig 13. B: In this experiment, we increased the concentrations of the cDNA and the Quantifiers, as well as the percentage of the gel to 16%, to visualise the small fragments of cDNA, such as the cDNA 2 (15-mer). However, even with these modifications, we could only observe bands corresponding to the 85-mer aptamer.

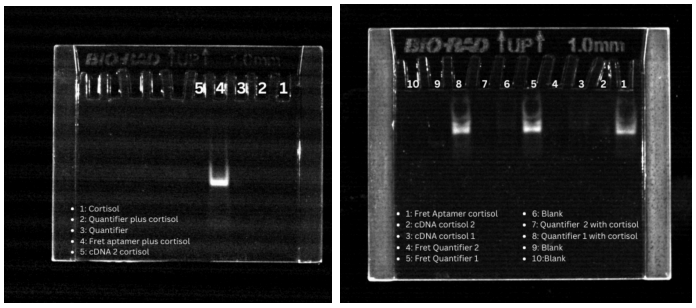

Figure 6: (A) Native PAGE with cDNA 1 and 85-mer cortisol aptamer (B)Native PAGE with both cDNA 1 and 2 and 85-mer cortisol aptamer.

Isothermal Titration Calorimetry

This experiment aimed to detect the hybridised complex of cDNA and aptamer.

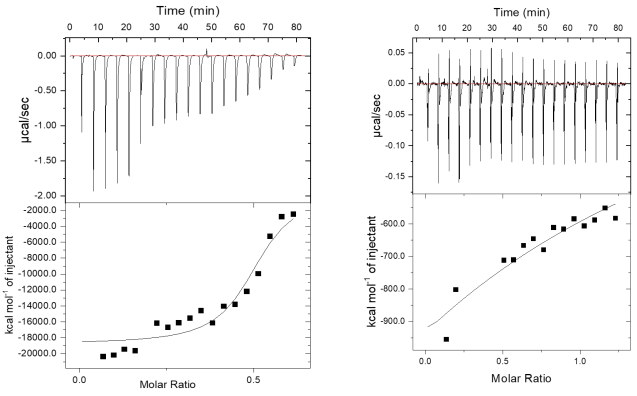

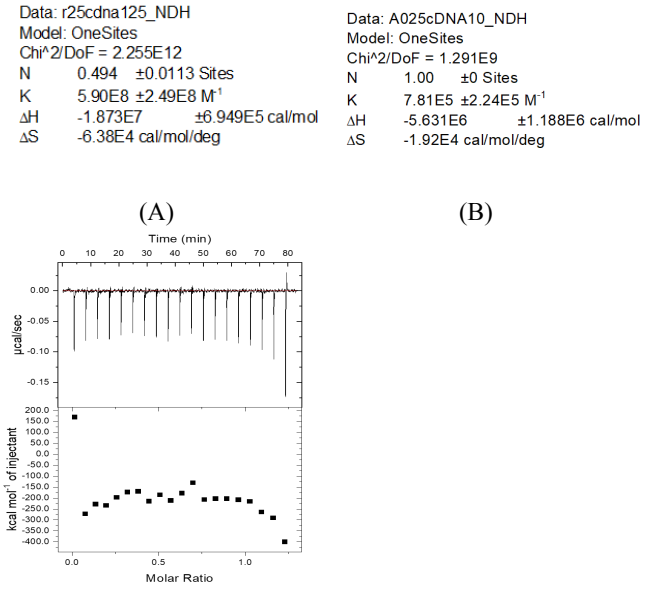

Figure 7: (A) ITC final graph depicting serotonin aptamer and cDNA1 serotonin binding: and respective parameters (B) ITC final graph 85-mer cortisol aptamer and cDNA1 cortisol; and corresponding parameters (C) ITC final graph 44-mer serotonin aptamer and cDNA1 serotonin.

As seen from the ITC result in Fig 7.A, there is a strong association between cDNA1 and the 44-mer serotonin aptamer.

Observing Fig 7.B, the relationship between the cortisol cDNA1 and the 85-mer aptamer was studied. The sigmoid shape suggests that the two molecules interact with each other.

This result could be strengthened by using a higher concentration of cDNA, as more molecules would be available to bind to the aptamer. This would lead to more complete binding in fewer injections and would, therefore, make the relationship between the two molecules more apparent. To test this hypothesis, we would need to conduct further experiments using different concentrations of cDNA and measuring the binding between the cDNA and the aptamer.

The duplex formation between the 44-mer serotonin aptamer and 12-mer cDNA2 was also studied (Fig 7. C). The results of the ITC experiment show that there is no obvious interaction between cDNA2 and the 44-mer serotonin aptamer. This result is consistent with the results of the fluorescent-based hybridisation experiments shown below.

Fluorescence-based experiments

Finding Ideal molar ratios: The initial concentration for each aptamer was determined by testing various concentrations ranging from 0.1 micromolar to 0.5 micromolar, to find the minimal concentration of aptamer that gives a detectable fluorescence. Details of finding the ideal initial concentration can be found in the supplementary material.

An initial concentration of 0.25 micromolar was used for 85-mer aptamer and the 44-mer serotonin aptamer, and an initial concentration of 0.5 micromolar for the truncated cortisol aptamer. To determine the ideal molar ratio for forming our aptasensor, We observed the difference in fluorescence intensity at t=0 (before binding) and t=60 mins (after binding).

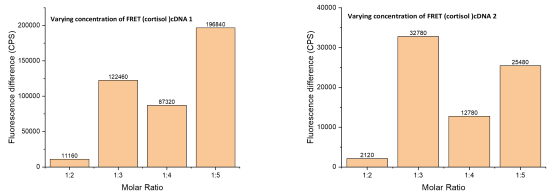

(A) (B)

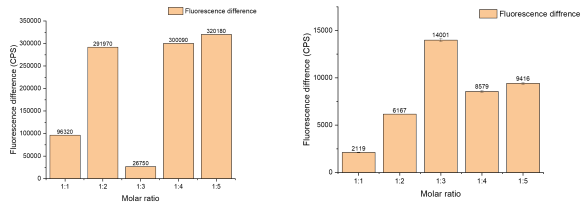

(C) (D)

Figure 8: (A) Varying molar ratios of 85-mer aptamer and cDNA1, (B) Varying molar ratio of 85-mer aptamer and cDNA2. (C) *Varying Molar ratios of truncated cortisol aptamer: cDNA, (D)Varying Molar ratios of 44-mer serotonin aptamer and cDNA 1*

From Fig 8.A, the ideal molar ratio for 85-mer cortisol aptamer and cDNA1 was observed to be 1:3 and 1:5. For the 85-mer cortisol aptamer and cDNA2 the ideal molar ratio was observed to be 1:3. From the Fig 8.C, for the truncated cortisol aptamer and cDNA, the ideal molar ratio was decided to be 1:2 because similar fluorescence differences were seen for 1:4 and 1:5. From Fig 8.D, the ideal molar ratio of 44-mer serotonin aptamer to cDNA 1 serotonin was observed to be 1:3.

Finding the ideal Hybridization time: The ideal hybridisation time and the quenching efficiency of the FRET system (fluorophore-quencher pair) for different molar ratios was determined by plotting the Ft/F0 values against time, using data from the fluoro spectrometer and plate reader.

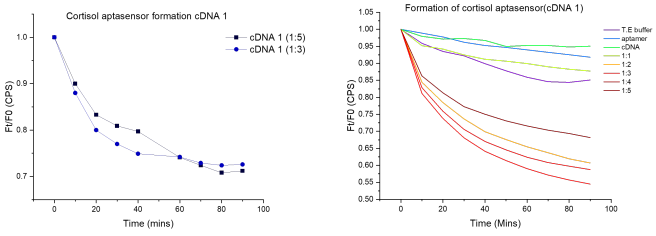

(A) (B)

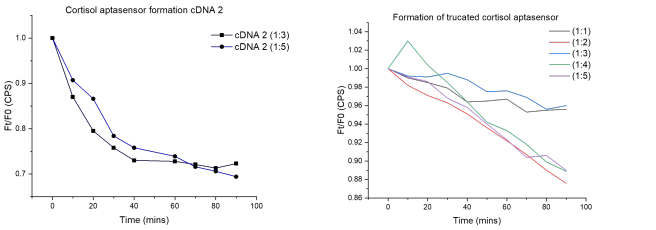

(C) (D)

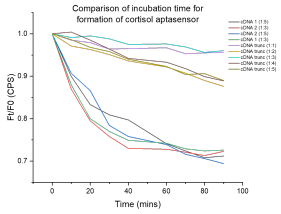

(E)

Figure 9 : (A) Cortisol aptasensor formation (85-mer aptamer & cDNA1) - fluorolog data (B) Cortisol aptasensor formation (85-mer aptamer & cDNA1) - microplate reader data (C) Cortisol aptasensor formation (85-mer aptamer & cDNA2) - fluorolog data (D) Cortisol aptasensor formation (truncated 14-mer aptamer & cDNA2) - fluorolog data (E)Comparison of cortisol aptasensor formation

From the data points obtained in the graph Fig 9.A, the ideal hybridization time for 1:3 molar ratio of 85-mer aptamer to cDNA 1 complex is around 50-60 minutes, where the graph plateaus. The maximum quenching of the donor fluorophore was achieved within 30 minutes of the hybridisation reaction.

This data was also replicated using a 1:5 molar ratio of the 85-mer aptamer to cDNA 1 complex. The 1:3 molar ratio was found to be much more effective in forming the duplex due to the shorter hybridization time required to reach the plateau level of Ft/F0.

The cortisol aptasensor formation was also tested with varying molar ratios ranging from 1:1 to 1:5, using T.E. buffer to prepare the oligos aliquots instead of milliQ (Fig 9.B). From this graph, we were able to reproduce the ideal hybridisation time of 60 minutes as seen from the fluorolog data. Upon examining the quenching outcomes, it is evident that the 1:3 molar ratio exhibits the highest quenching, approximately 45%, which aligns with our previous molar ratio results. The elevated quenching capability, rising from 30%, as indicated in the fluorolog data, to 45%, could potentially be attributed to the use of T.E buffer instead of milliQ.

Fig 9.C shows the results of a fluorescence experiment to measure the hybridisation time of an 85-mer aptamer to cDNA 2. The graph shows that the ideal hybridization time is around 50-60 minutes for both the 1:3 and 1:5 molar ratios. Maximum quenching of the fluorophore is achieved within 30 minutes of the hybridisation reaction, in both cases. This suggests that the molar ratio of the aptamer to cDNA 2 does not significantly affect the hybridisation time.

The hybridisation time and the quenching capacity have similar trends across both the cDNA that was designed for the 85-mer aptamer sequence.

Formation of cortisol aptasensor from truncated aptamer and cDNA: From Fig 9.D, we can see that no plateau has been reached even after running the experiment for 90 mins and the maximum quenching efficiency observed is around 12% which is seen by 1:2 molar ratio again aiding our result obtained from the molar ratio graph.

Comparing the various possible cortisol aptasensors to determine the best cDNA-aptamer pair: Figure 9.E shows that the truncated cDNA and aptamer complex does not produce a very efficient FRET system. This is likely because the truncated cDNA is shorter and has fewer binding sites for the aptamer. Additionally, the graph shows that cDNA 1 and cDNA 2 produce similar results in terms of hybridization time and quenching efficiency, regardless of whether they are complexed with the 85-mer aptamer. This suggests that the

binding affinity of the aptamer for cDNA 1 and cDNA 2 is similar. The overall results of this experiment suggest that the truncated cDNA and aptamer complex is not a very good candidate for developing an aptasensor. The quenching efficiency is too low, and the hybridization time is too long. The 85-mer aptamer, along with cDNA 1 and cDNA2, are better candidates for developing an aptasensor.

Formation of serotonin aptasensor from 44-mer aptamer and serotonin cDNA1:

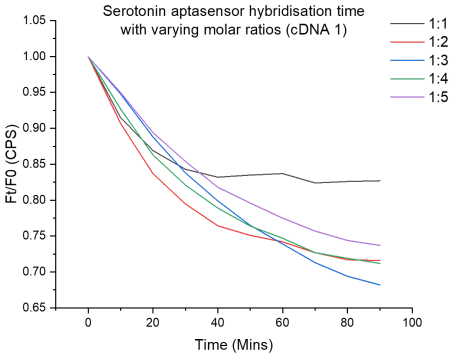

Figure 10 : Serotonin aptasensor formation (44-mer serotonin aptamer & cDNA 1)

We performed this experiment to determine the ideal molar ratio and hybridisation time for forming a serotonin aptasensor. We used a microplate reader to measure the fluorescence intensity of the aptasensor at different molar ratios of aptamer:cDNA. We performed multiple technical replicates and three experimental replicates to ensure the accuracy of our results. The ideal hybridisation time for the serotonin aptasensor is observed to be around 50-60 minutes, which is similar to the ideal hybridisation time for the cDNA cortisol aptamer complex. The quenching efficiency of the serotonin aptasensor is around 30% at a 1:3 molar ratio of serotonin to the aptamer. This is consistent with the prediction that a 1:3 molar ratio is ideal for forming the serotonin aptasensor. The lowest quenching efficiency was observed at a 1:1 molar ratio of serotonin to aptamer, which was around 15%. The quenching data is supported by the ITC report, which shows that there is high affinity between the cDNA 1 and serotonin aptamer.

Formation of serotonin aptasensor from 44-mer aptamer and serotonin cDNA 2:

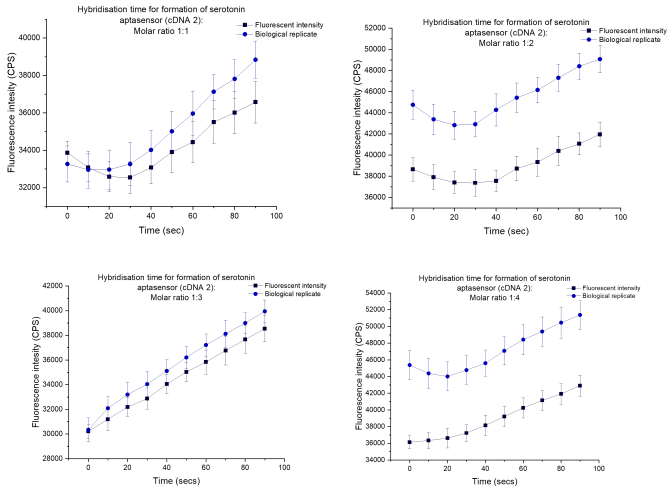

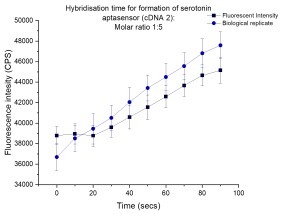

Figure 11

From the above graphs we can observe that there is an increase in fluorescence upon apparent hybridisation of the cDNA 2 and serotonin aptamer oligos for all molar ratios. This trend was also observed in the replicate data, which is plotted on the same graphs. Multiple technical replicates were also performed, as shown by the standard deviations plotted with both the first and replicate data points. This data is further justified by the ITC plot we obtained for cDNA 2 and serotonin aptamer which showed that there was no significant association between cDNA 2 and serotonin aptamer.

Sensitivity experiments:

The sensitivity of an aptasensor is its ability to detect small changes in the concentration of the target molecule or biomarker. To test the sensitivity of the aptasensor, we used the ideal aptasensor that had been determined in previous experiments. Next, we measured the increase in fluorescence obtained upon adding varying concentrations of our biomarker mimicking the human physiological value.

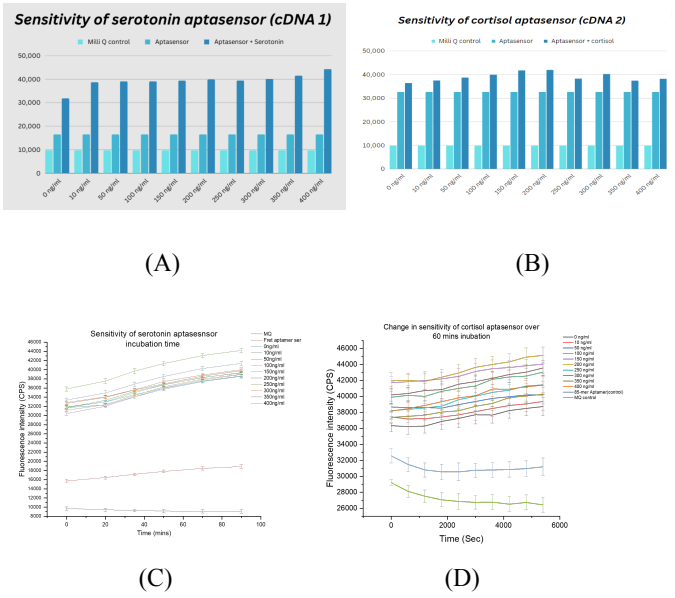

Figure 12 : (A) Sensitivity of serotonin aptasensor (B) Sensitivity of cortisol aptasensor (C) Change in fluorescence over time upon addition of varying concentration of serotonin (D) Change in fluorescence over time upon addition of varying concentration of cortisol with cortisol aptasensor.

Sensitivity of serotonin aptasensor:

Serotonin concentration (ng/ml)	0	10	50	100	150	200	250	300	350	400
Fold change wrt to aptasensor + 0ng/ml	1	1.216	1.277	1.288	1.237	1.253	1.238	1.260	1.303	1.392

These data points were taken after 60 mins incubation of the aptasensor and serotonin. The fold change in fluorescence is calculated by dividing the fluorescence of the aptasensor with serotonin by the fluorescence of the aptasensor without serotonin, comparing results at different serotonin concentrations. The fluorescence increases with increasing concentrations of serotonin indicates that the aptasensor can be used to quantify serotonin levels. Although we didn't expect an increase in fluorescence upon adding milliQ to our aptasensor, the increase observed upon the addition of varying concentration of serotonin showed a greater fluorescence reading. Taking this into consideration, we indicated the fold change wrt to aptasensor + 0ng/ml and, therefore, we can reliably correspond the fold change to a particular serotonin concentration mimicking human physiological levels present in the human serum.

From Fig 12.C we can see that the controls such as milli Q show a decrease in fluorescence as time increases but the aptasensor plus cortisol for varying concentrations shows a trend of increase in fluorescence as time increase, which is visible in multiple technical replicates. This shows that the aptasensor loses its cDNA strand which causes its increase in fluorescence due to loss of the FRET system.

Sensitivity of cortisol aptasensor:

Cortisol concentration (ng/ml)	0	10	50	100	150	200	250	300	350	400
Fold change wrt to aptasensor + 0ng/ml	1	1.03	1.07	1.10	1.15	1.16	1.05	1.06	1.03	1.05

The sensitivity tests were done using cDNA 2 and 85-mer cortisol aptamer to form the ideal aptasensor since both cDNA 1 and cDNA 2 showed similar trends for the formation of aptasensor (Fig 12.B). From the result shown we can derive that the cortisol aptasensor shows higher sensitivity from the range of 50ng/ml to 200 ng/ml, which lies well in the range of human physiological serum levels of cortisol.

Fig 12.D shows that the fluorescence of the controls (aptasensor and milliQ) decreases over time, but the fluorescence of the aptasensor with varying concentrations of cortisol increases over time, indicating the displacement of the aptamer and cDNA strand. This trend is visible in multiple technical replicates, which confirms that it is not a one-off event.

Sensitivity experiments were also conducted on a truncated cortisol aptamer in order to validate our chosen cortisol aptasensor formed using cDNA 2. The results can be found in the supplementary material.

In conclusion, we measured fold change with respect to aptasensor + 0ng/ml for the serotonin and cortisol aptasensor and for the serotonin aptamer, we could observe a functional relationship with an increase in serotonin concentration but we found the cortisol aptasensor to show higher sensitivity from the range of 50ng/ml to 200 ng/ml which lies well in the range of human physiological serum levels of cortisol.

Specificity experiments

From these experiments, we aim to find the effectiveness of the turn-on mechanism upon interaction with the specific biomarker, in this case, serotonin. Experiments were done to check the effectiveness of the serotonin aptasensor in a mixture of biomarkers.

To check the specificity of our aptasensor we conducted a biomarker mix test where we tested the specificity of our serotonin aptasensor by checking its rise in fluorescence upon the addition of various different biomarkers other than serotonin and a mixture of all the biomarkers: If our aptasensor is specific, the increase in fluorescence upon addition of other biomarkers other than serotonin should show a reduced increase in fluorescence compared to the increase obtained when bound to serotonin. This increase should also be visible when the aptasensor in exposed to the mixture of biomarkers.

The fluorescence difference shown in Fig 13 is fluorescence measured at time t = 90 mins minus the fluorescence at time t = 0 mins. We observed that the serotonin aptasensor showed a greater fluorescence difference when placed in addition to the serotonin biomarker and the mixture of biomarkers compared to its difference in the presence of other biomarkers. Hence, this proves that our serotonin aptasensor is specific. An even greater difference is observed in the biomarker mix data but this is expected because the excess fluorescence could be due to the background signal seen in the presence of other biomarkers as shown in the graph.

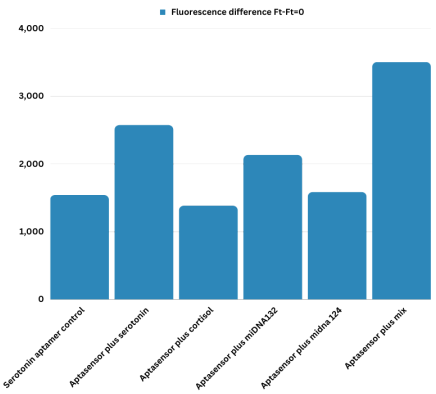

Figure 13 : Specificity of serotonin aptasensor

In conclusion, we observed that the serotonin aptasensor showed a greater fluorescence difference when placed in addition to the serotonin biomarker and the mixture of biomarkers when compared to its difference shown in the presence of other biomarkers. Hence this proves that our serotonin aptasensor is specific in nature.

Gsα protein

Our plans for Gsα protein included expression, purification of protein and quantification by aptasensors. We intended to synthesise an aptamer for the Gsα protein using the SELEX (Systematic Evolution of Ligands by Exponential Enrichment) method to select the aptamers that bind specifically to the Gsα Protein.

Unfortunately, due to time and budget constraints, we were unable to procure and work with the aptamers. Our cloning experiments are documented here, and our future protocols regarding the purification and formation of aptasensors can be found in the supplementary material. The Gsα Gblock was procured through IDT.

Gradient PCR: We did a PCR reaction to amplify the Gsα Gblock. In order to confirm the annealing temperature, we ran a gradient PCR. The protocols for the same can be viewed in the supplementary material.

From Fig14.A, the tubes H, I, J, K, and L were annealed at different temperatures along with positive control. The bands were found to be most visible in lanes K and L. The optimum temperature for successful amplification was found to be at 62.5 degrees Celsius.

PCR amplification was performed again with the right annealing temperature (Fig 14.B)

Restriction Digestion: After overnight restriction digestion, we ran an agar gel with the Gsα Gblock and PET 19b Plasmid. We used two positive controls, a gene fragment of 1.5kb and our amplified Gsα Gblock (1.2kB).

The second band was observed to be around 1kb, confirming the formation of a restriction-digested insert of 1198bp size. Third band is observed between the 5kB and 6kB bands of the ladder, confirming the presence of a restriction-digested vector. The presence of a single band confirms the successful restriction digestion of the pET19B (5.7kB) vector. Bands are not visible for the positive controls (Fig 14.C)

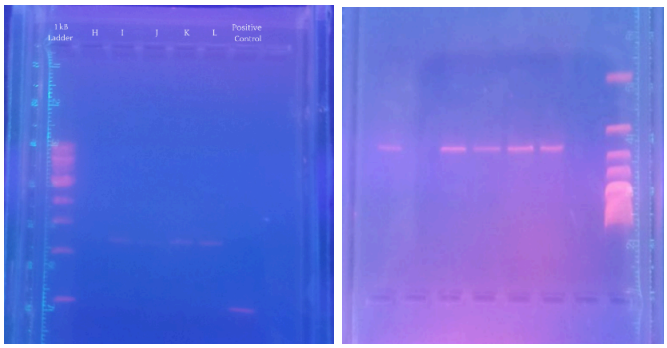

(A) (B)

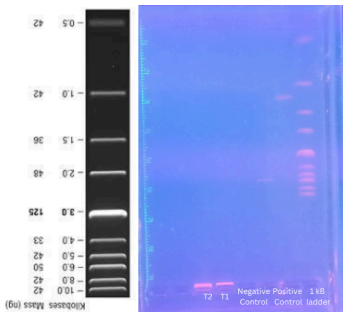

(C)

Figure 14: (A) Gradient PCR under Trans Illuminator (B) PCR amplification of Gsα Gblock (C) Gel after restriction digestion

Ligation: A ligation reaction was set up with a reverse and backward primer and a T4 DNA ligase. When further transformation experiments were carried out, 2 colonies were obtained. A master plate was made, and a colony PCR was performed, which did not yield successful results. The possible reasons for ligation PCR not giving desirable results could be due to the machine being faulty. Due to time constraints, we could not troubleshoot the protocol and further experiments for the Gsα Gblock.

Hardware

To determine the sensitivity of the photodarlington sensor

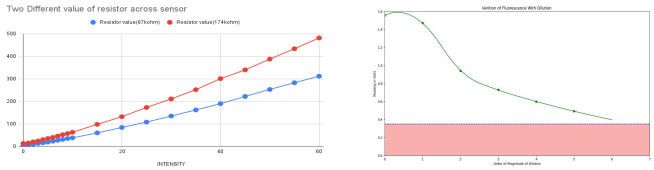

Figure 15: (A) Results of an experiment with different values of resistors across the sensors (87 komh and 174kohm) and increased the LED intensities plotted graphically (B) A calibration curve is obtained by plotting output voltage versus the PTE concentration to create a calibration curve.

Firstly, we measured the output voltage of the sensor at different light intensities from a green LED (Fig 15.A) Secondly, we moved on to a real lab sample, where we measured the output voltage of the sensor when exposed to different concentrations of PTE (phenyl tetraene) in DCM (dichloromethane) (Fig 15.B)

Lastly, we immobilised the biomarker on our aptasensors and our nanoprobe and then measured the output voltage of the sensor when exposed to different concentrations of the Biomarker bound with the aptasensor. We again plotted the output voltage versus the biomarker concentration to create a calibration curve.

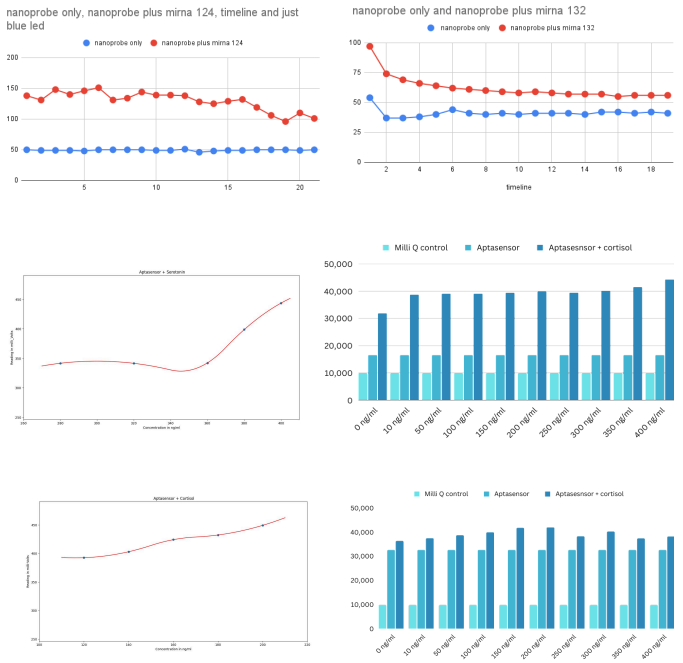

Figure 16: (From the top) (A)Nanoprobes (B) Aptasensor and serotonin (C) Aptasensor with cortisol.

Fig 16.A shows the Arduino value vs time graph for the experiment with nanoprobe alone and with two different miRNAs 124 and 132 over time. Fig 16. B shows the graph for different concentrations of serotonin with the aptasensor, when compared in the same range of

concentration, the functional form of the maximas of the histograms match well with the interpolated form of fluorimeter readings and Rudimentary analysis on the ratio of change also matches however more investigation has to be done. Fig 16.C shows the graph for different concentrations of cortisol with the aptasensor, when compared in the same range of concentration, the functional form of the maximas of the histograms matches well with the interpolated form of fluorimeter readings and Rudimentary analysis on the ratio of change also matches however more investigation has to be done.

Conclusion

We have successfully developed a set of quantifiers that could detect and quantify the biomarkers in physiological concentration with high specificity. We have built a detector unit and a prototype for the microfluidic chip. The portable and budget-friendly nature of the detector unit vastly increases its acceptability as a tool. The promising results obtained from the quatifier data give high hopes for actual tests on blood samples in the near future.

Future Directions

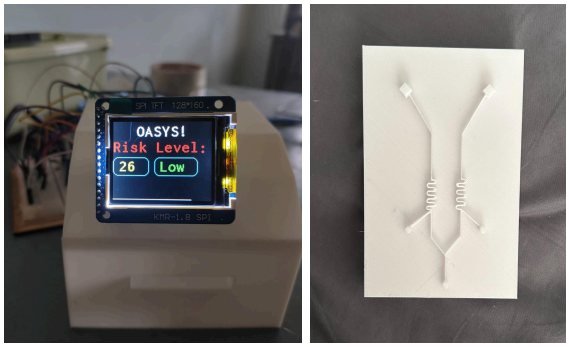

Figure 17 : (A) Hardware (B) 3D printed mould of the microfluidic chip

In this section, we will briefly outline the experiments needed to optimise OASYS as a functional system further. For this project we utilised synthetically procured sequences of miDNA to mimic conditions in blood. Rigorous rounds of testing and experimentation will be required to replicate these results in miRNAs and human blood samples.

Temperature-based assays: Running the hybridisation fluorescence-based experiments for the formation and sensitivity of our aptasensors in varying temperatures will provide us with optimal temperature conditions for increased sensitivity of the aptasensor. They can also help determine the optimal temperatures for aptamer binding and aptasensor formation.In addition, temperature-based assays can also be used to study the thermodynamics of aptamer binding to design aptasensors with improved binding affinity and stability.

ITC experiments for nanoprobe: Isothermal Titration Calorimetry (ITC) can distinguish between multiple binding sites with different affinities on the same molecule, thus it can prove binding of three different hybridizing sequences together to form the probe. By comparing ITC data from experiments conducted with modified DNA sequences or conditions, it's possible to probe the role of specific bases or structural elements in the binding interaction. This can help in understanding the molecular basis for specificity or the role of certain regions in DNA binding.

Protein Expression and Purification: We intend to complete Gsα protein expression and purification. Further experiments would include Sanger sequencing to confirm the transformed sequence and performing SELEX to obtain specific aptamers.

Hardware: Moving forward, we are considering a transition from the current Arduino UNO to the ESP32 microprocessor series. There is a significant upgrade in the allowed memory (2 KB RAM to 520 KBRAM, 32 KB flash memory to 4 MB flash memory) allowing us to expand our product to include more photosensors and modules, as well as add more complex programming structures and functions. ESP32 boards have built-in WiFi and Bluetooth, allowing us to connect them to a user-friendly app or website. They can also run Python and TensorFlow, enabling machine learning on the device. This means that the product can measure data, collect it to a server, analyze it with machine learning, and optimize itself for any demographic. All these advantages come along with the point that currently, the ESP32 board is ~20% cheaper than the Arduino, which is a key factor as our primary goal is humanitarian and to make the product affordable, even in developing or third-world countries. We will also design a compact circuit board layout to minimise the device's size. We are considering changing the measurement from voltage to capacitor discharge time, which would allow us to measure very low currents accurately.

Microfluidics: Our current constructed design is only a two-channel chip containing one quantifier of each type to test the validity of our quantifier-biomarker system. We are in the process of designing the five-channeled microfluidic chip that can process all five of our biomarkers but requires much refining to be used for testing. We also plan to leave the domain of prototyping and enter the market as a tool that can be sold, for which we have several important steps that we would like to include in our microfluidics chip, like a Finger Actuated Pressure system to reduce the hassle of using complicated pumps and syringes in the chip as much as possible, and also creating a manufacturing mould for scaled manufacturing of the chip so that it can be market ready. We were helped by CCAMP in Bangalore to plan this out for our future market endeavours.

Software: One of the primary functions of the microfluidic chip is to analyse biomarker data obtained from blood samples and provide a degree of risk for clinical depression. This risk assessment will be based on complex algorithms and statistical analysis of the biomarker data. We will continuously refine the algorithms used for risk assessment. This iterative process will involve incorporating newly discovered biomarker data, whether from our tool or independently, and improving the accuracy of our quantification system.

Materials and Methods

Native PAGE

A native PAGE (polyacrylamide gel electrophoresis) was chosen to verify that our complementary sequences formed the probe and demonstrate that our miDNA can bind to the probe. We used a 12 per cent gel, and the polyacrylamide solution was in a 1:19 ratio of acrylamide to bisacrylamide. The 12 per cent gel could distinguish a 22 nucleotide difference in the sample.

The native PAGE ensures that the base pairing between the complementary strands remains intact during the electrophoresis, which is required to verify the formation of our probe. The experiment used standard SDS PAGE equipment, but a longer gel is ideal.

Dynamic light scattering

The zeta potential analyser was used to find if the nanoparticles were evenly distributed in the solution and to confirm the presence

of stable carboxylic acid groups. This system is designed to characterise colloidal, nanoparticulate, and macromolecular samples. It can determine the zeta potential, which measures the electrostatic potential at the interface between a particle and the surrounding liquid or dispersion medium.
The instrument works based on Dynamic Light Scattering (DLS). It will detect the fluctuation in the intensity of scattered light over a period caused by the Brownian movement of particles and can calculate the zeta potential with this reading.

A singular peak in the resulting graph would mean that the particles are well dispersed in the medium. A zeta potential value, lower than -20 mV, will indicate that stable carboxyl groups are present in the solution.

Transmission Electron Microscopy
To obtain high-resolution images of our nanoparticles for size determination, we conducted Transmission Electron Microscopy (TEM) studies. TEM is a microscopy technique that transmits a beam of electrons through a thin specimen and captures the transmitted electrons to create high-resolution images. The sample must be loaded on a copper grid and air-dried to remove all the excess water.

Microplate reader for fluorescence studies
All the experiments mentioned below were performed on a Costar, black, flat-bottom plate. The readout was taken by performing an emission scan, with a constant excitation of 490 nm and emission range of 500 to 600 nm, with readings taken in 1 nm steps.

Fluorolog for fluorescence studies
All the experiments mentioned below were performed on a Greiner 96 Flat Bottom Transparent Polystyrene Cat. No.: 655101/655161/655192 [GRE96ft.pdfx] plate. The FluoroLog fluorometer is a versatile instrument that can measure the fluorescence of a wide variety of samples. It is important to follow the protocol carefully to ensure accurate and reproducible results…
+
Isothermal Titration Calorimetric Experiment
Isothermal titration calorimetry (ITC) is a powerful technique for measuring biomolecular interactions' thermodynamics, including DNA duplexes' formation. It gives direct measurement of thermodynamics, enables label-free detection and is highly sensitive. ITC experiments are performed at a constant temperature, so the heat measured is directly proportional to the change in enthalpy of the binding reaction. During an ITC experiment, a ligand solution is titrated into the sample cell. The heat released upon binding of ligands to biomolecule is detected by the calorimeter and recorded as a thermogram. The thermogram is a plot of the heat released or absorbed as a function of the amount of ligand added.

The thermogram can be analyzed to determine the following thermodynamic parameters of the binding reaction; Binding affinity (K_A): The strength of the interaction between the ligand and the biomolecule, Enthalpy (ΔH): The amount of heat released or absorbed during the binding reaction, Entropy (ΔS): The change in disorder of the system during the binding reaction and Stoichiometry (n): The number of ligand molecules that bind to each biomolecule.

To check duplex formation between an aptamer and corresponding cDNA, We prepared a 0.25 micromolar concentration solution of the aptamer and titrated it against 1 micromolar concentration of cDNA. The reference cell contained the same Milli-Q water we used to prepare our working concentration. 1.5 microliters of injection were given every 80 seconds for 20 injections

Cloning
dsDNA gBlock fragments coding for GNAS was obtained from Twist Bioscience and designed using SnapGene software with an Nde1 site upstream and BamH1 site downstream. Primers were also designed on SnapGene. PCR amplification of the gene fragments with a high-fidelity polymerase was carried out, followed by restriction digestion by Nde1 and BamH1. The double digested backbone with cohesive ends was ligated with the digested inserts by the T4 DNA ligase and the mixture was transformed into *E. coli* DH5a. Positive transformants were screened by colony PCR.

Detailed protocols for PCR, restriction digestion, PCR cleanup, gel extraction, ligation, transformation, colony PCR, Sanger sequencing and plasmid isolation can be found in the supplementary material.

Biosafety

The degradation products of Polydimethylsiloxane (PDMS) do not significantly affect soil microbes, animals, or crops. PDMS also do not bioaccumulate. Both the aptasensors and the nanoprobes can quantify the biomarkers at physiological concentrations without using enzymes, thereby avoiding the risk of enzymes accidentally leaking and causing discomfort to the user. Leakage preventive valves ensure that the blood that enters the device does not leak out because of backflow and cause contamination. The material used to make the shell of our detector unit (Polylactic acid (PLA) is biodegradable as well as recyclable.

Data and References

1) Tolentino, J. C., & Schmidt, S. L. (2018). DSM-5 Criteria and Depression Severity: Implications for Clinical practice. *Frontiers in Psychiatry*, *9*. https://doi.org/10.3389/fpsyt.2018.00450
2) Depressive disorder (depression)
3) Global burden of mental disorders and the need for a comprehensive, coordinated response from health and social sectors at the country level
4) Joseph, J., Sankar, D. H., & Nambiar, D. (2021). The burden of mental health illnesses in Kerala: a secondary analysis of reported data from 2002 to 2018. *BMC Public Health*, *21*(1). https://doi.org/10.1186/s12889-021-12289-0
5) Major Depressive Disorder - StatPearls - NCBI Bookshelf
6) Pehlivan, Z.S., Torabfam, M., Kurt, H. *et al.* Aptamer and nanomaterial based FRET biosensors: a review on recent advances (2014–2019). *Microchim Acta* **186**, 563 (2019). https://doi.org/10.1007/s00604-019-3659-3
7) Tian, H., Yuan, C., Liu, Y., Li, Z., Xia, K., Li, M., Xie, F., Chen, Q., Chen, M., Fu, W., & Zhang, Y. (2020). A novel quantification platform for point-of-care testing of circulating MicroRNAs
8) based on allosteric spherical nanoprobe. *Journal of Nanobiotechnology*, *18*(1). https://doi.org/10.1186/s12951-020-00717-z